RESEARCH

Flue gas analysis for biomass and coal co-firing in fluidized bed: process simulation and validation

Daulet Zhakupov[1] · Lyazzat Kulmukanova[1] · Yerbol Sarbassov[1] · Dhawal Shah[1]

Abstract
Coal-conversion technologies, although used ubiquitously, are often discredited due to high pollutant emissions, thereby emphasizing a dire need to optimize the combustion process. The co-firing of coal/biomass in a fluidized bed reactor has been an efficient way to optimize the pollutants emission. Herein, a new model has been designed in Aspen Plus® to simultaneously include detailed reaction kinetics, volatile compositions, tar combustion, and hydrodynamics of the reactor. Validation of the process model was done with variations in the fuel including high-sulfur Spanish lignite, high-ash Ekibastuz coal, wood pellets, and locally collected municipal solid waste (MSW) and the temperature ranging from 1073 to 1223 K. The composition of the exhaust gases, namely, $CO/CO_2/NO/SO_2$ were determined from the model to be within 2% of the experimental observations. Co-combustion of local MSW with Ekibastuz coal had flue gas composition ranging from 1000 to 5000 ppm of CO, 16.2%–17.2% of CO_2, 200–550 ppm of NO, and 130–210 ppm of SO_2. A sensitivity analysis on co-firing of local biomass and Ekibastuz coal demonstrated the optimal operating temperature for fluidized bed reactor at 1148 K with the recommended biomass-to-coal ratio is 1/4, leading to minimum emissions of CO, NO, and SO_2.

Keywords Biomass cofiring · Fluidized-bed combustion · Advanced process simulation · Flue-gas emissions · Fuel utilization · Aspen plus

List of symbols

GHG	Greenhouse gas
CFD	Computational fluid dynamics
FBR	Fluidized bed reactor
MSW	Municipal solid waste
FC	Fixed carbon
VM	Volatile matter
CSTR	Continuous stirred-tank reactor
HHV	Higher heating value
TDH	Transport disengagement height
B	Biomass
C	Coal
ρ_g	Density of a gas
ρ_s	Density of solids
μ	Viscosity
Ar	Archimedes number
d_p	Diameter of a particle
E_{Ai}	Activation energy of reaction i
H_{mf}	Height of bed at minimum fluidization
k_i	Pre-exponential factor of reaction
n_i	Temperature exponent
Re_{mf}	Reynolds number at minimum fluidization velocity
r_i	Reaction rate of reaction i
u	Operating velocity
u_{mf}	Minimum fluidization velocity
u_{or}	Velocity through the orifice
ΔP_b	Pressure drop over bed
ΔP_d	Pressure drop over distributor plate
g	Acceleration of gravity
φ	Sphericity of particles
ε_{mf}	Voidage at minimum fluidization

✉ Dhawal Shah
    dhawal.shah@nu.edu.kz

1   Department of Chemical and Materials Engineering, School
    of Engineering and Digital Sciences, Nazarbayev University,
    010001 Nur-Sultan, Kazakhstan

1 Introduction

Coal-fired energy processes continue to be the dominant energy sources around the world in the era of rapid urbanization and economic growth. According to the International Energy Agency, 38.5% of the total energy generation in the

world is produced by coal (IEA 2018). Despite the maturity of the technology, coal conversion has a negative reputation due to the adverse impact on the environment (Kerimray et al. 2018; Peters et al. 2020). For countries such as Kazakhstan, wherein coal-combustion segment takes the highest portion in the energy mix, environmental consequences such as greenhouse gas (GHG) emissions, air deterioration, soil contamination as a result of ash landfilling, are particularly notable. Even though countries are preparing for the shift in the energy sector towards environmentally friendly energy sources, it is still important to consider that the shift cannot occur instantaneously and therefore a need emerges for optimization of existing coal conversion. As a member of the Paris Agreement, Kazakhstan has declared to reduce 25% of the national GHG emissions by 2030 compared to the level of 1990 (UNFCCC 2011).

Biomass is a carbon–neutral fuel and considering the overall life-cycle, biomass conversion has a potential to be a carbon negative process (Sher et al. 2018). Co-firing of coal with biomass also claims to reduce emissions of SO_x and NO_x due to low content of sulfur and nitrogen in the biomass (Kumar et al. 2018), while maintaining a comparable heating value (Roni et al. 2017). Experiments conducted by Kommalapati et al. (2018), demonstrated a decrease in life cycle emissions for CO_2 (by 13.45%) and NO_x (by 11.70%) for the blend fuel with 15% of biomass. However, along with advantages, certain technical issues of biomass/coal co-firing, such as growth of soot deposition in the reactor, ash composition, and morphology changes, needs to be considered (Kumar et al. 2018; Bhuiyan et al. 2018). In addition, limited literature is available on comprehensive analysis of efficient integration of biomass into existing coal firing systems. Even though biomass has a great capacity in the energy sector, especially when coupled with coal, increased cost of operation and pretreatment for biomass fuel brings challenges to quick fuel integration (Khan et al. 2009; Roni et al. 2017; Lawal et al. 2021). Therefore, an understanding of the behavior of the conversion process at different biomass to coal ratio in blended fuel is of current interest.

Optimization through modelling requires thorough analysis and validation. Most of the coal/biomass combustion models in the literature are built on Computational Fluid Dynamics (CFD), using Eulerian–Eulerian or Eulerian–Lagrangian approach. The approach often takes into consideration combustion reaction kinetics and reactor hydrodynamics, as a part of holistic modelling (Lawal et al. 2021; Bi et al. 2021; Adamczyk et al. 2015). However, results based on the CFD models strongly depend on the grid selection and assumption, including improper modeling of the complex momentum equations. In addition, the simulation using CFD cannot be referred to as a user-friendly approach for optimization execution (Xie et al. 2014; Žnidarčič et al. 2021). Another modeling approach

mentioned in the literature involves utilization of Aspen Plus® software. Being one of the leading chemical process modeling software, Aspen Plus incorporates various attributes required for comprehensive process modeling along with the user-friendly interface. However, limited studies are available for coal/biomass co-firing processes models built in Aspen plus, especially the ones occurring in Fluidized Bed Reactor (FBR) unit. Complex hydrodynamics of the combustion reactor and chemical reaction kinetics bring some challenges to the models and their optimization.

Earlier models developed in Aspen Plus for simulation of the fuel combustion in FBR have, in general, a limited set of reactions and were governed by simple reaction kinetics. For instance, Yang et al. (2011) have built a model using 16 combustion reactions; however, the model was specifically focused on NO and N_2O prediction. In addition, in their model formation of the SO_x was neglected, and tar was considered as an inert material. In another study by Hu et al. (2018), the model incorporated six reactions with a focus on full carbon oxidation and char combustion. At the same time formation of NO_x and SO_x gases were not considered in this particular study, as well. More recent model for the sewage sludge thermal decomposition in an FBR unit by Fedorov et al. (2021), adapted a simple reaction kinetics. In particular, seven reactions were considered for carbon conversion into carbon monoxide with a further oxidation to carbon dioxide. In the model, the authors simulated FBR using RGibbs equilibrium reactor. This equilibrium reactor neglects the effect of the hydrodynamics and fluidization on the reactor performance. According to the authors, coal and wet sewage sludge devolatilization products of the model were completely reacted. Altogether, even in the recent Aspen Plus-based models, combustion kinetics is simplified to basic carbon oxidation or NO_x predictions and/or the modelling of the FBR is performed using equilibrium reactors.

In our previous work, we simulated combustion of low-grade bituminous Ekibastuz coal utilizing the Aspen Plus using the fluid bed unit (Saparov et al. 2021). The model was validated using the experiments on a pilot-scale circulating fluidized bed (CFB) coal combustion. The comprehensive model included detailed hydrodynamics of the fluid bed unit. However, the combustion reaction was modeled by simple kinetics of carbon and hydrogen combustion and the effect of volatiles were neglected. Herein, we aim to expand the model to implement FLUIDBED unit with a broader reaction set including NO_x, SO_x and tar combustion including the effect of volatiles and further incorporate co-combustion of biomass and coal in the FBR unit.

The advancement in modeling aims to improve the dynamic operations of the process and maintain high efficiency of co-combustion (Zhou et al. 2011; Wu et al. 2017). In the following sections, the development of the model is discussed in

detail, followed by the validation using the well-established literature data provided by researchers (Varol et al. 2018; Peters et al. 2020) on co-firing of coal and biomass, and also with our previous experiments on Ekibastuz coal combustion. Lastly, sensitivity analysis is performed based on the available data for the Ekibastuz coal and organic fraction of MSW collected in Nur-Sultan. The scope of current research is to develop and validate the biomass co-combustion model using Aspen Plus and examine its adaptability with experimental data available in the literature.

2 Methodology

2.1 Process development

Combustion of the solid fuel particles in the fluidized bed reactors undergoes three key steps: drying, devolatilization/pyrolysis, and combustion, each of which is modeled separately in Aspen Plus (Liu et al. 2020a). The explanation of each step pathway is demonstrated in Table 1.

At drying and pyrolysis steps moisture entrapped in the fuel is evaporated (Aghaalikhani et al. 2019; Awasthi and Bhaskar 2019; Dwivedi et al. 2019). Further, pyrolysis proceeds with a decomposition of the dry fuel particles to volatiles, char, and ash. The composition of resulting compounds depends on the proximate analysis and operating conditions, as we discuss later. Lastly, devolatilization occurs wherein the obtained volatiles are disintegrated into tar, CH_4, CO, CO_2, H_2, H_2O, HCN, and NH_3 (Awasthi and Bhaskar 2019). In the current work, the composition of volatiles was calculated using the theory of the functional-group dependence on the ultimate analysis for coal (Serio et al. 1987). The selected approach is based on the experimental results for the volatile composition of six different coal types during pyrolysis that are shown in Table S1 in Supplementary Material. Using the data set, a linear regression was performed to obtain a separate equation for each volatile component as a function of structural elements (Table S2 in Supplementary Material). The data set consists of loosely coupled and tightly coupled molecules, like H_2O; however, these are combined together during the regression analysis.

Finally, the oxidation of the char and volatile gases in the reactor develops at 1123–1273 K. The combustion kinetics were adapted from several papers published on the burning of the pure coal/biomass and their mixtures, and the main criterion for the selection was the presence of the validation on the

experimental results (Serio et al. 1987; Zhou et al. 2011; Gu et al. 2020; Liu et al. 2020b). Table 2 demonstrates the reaction set utilized in the fuel combustion. Combustion reaction kinetics are included in Table S3 in the Supplementary Material.

2.2 Model assumptions

The model was designed considering the following assumptions:

(1) Drying and pyrolysis occurs instantaneously and the process is under steady-state.
(2) The temperature across the FBR is uniform.
(3) The produced tar is reactive, and the produced char is 100% carbon (Merrick 1984).
(4) Functional group distribution of volatiles is correlated to the ultimate analysis of the fuel.
(5) Coal and biomass have similar volatile components.
(6) Heat transfer throughout the process is not considered.

Instantaneous drying and pyrolysis can be justified by its relatively fast decomposition rates at high temperatures present in the FBR. Furthermore, the uniform temperature distribution in FBR has been observed, for example, by Zhou et al. (2011), wherein the riser temperature varied only

Table 2 Set of reactions involved in fuel combustion process in FBR

R_1	$CH_4 + 1.5\,O_2 \rightarrow CO + 2\,H_2O$
R_2	$H_2 + 0.5\,O_2 \rightarrow H_2O$
R_3	$H_2S + 1.5\,O_2 \rightarrow H_2O + SO_2$
R_4	$HCN + 0.75\,O_2 \rightarrow CNO + 0.5\,H_2O$
R_5	$NH_3 + 1.25\,O_2 \rightarrow NO + 1.5\,H_2O$
R_6	$NO + CO \rightarrow 0.5\,N_2 + CO_2$
R_7	$CO + 0.5\,O_2 \rightarrow CO_2$
R_8	$CNO + 0.5\,O_2 \rightarrow NO + CO$
R_9	$C + \left(\frac{1}{\Phi}\right)O_2 \rightarrow \left(2 - \frac{2}{\Phi}\right)CO + \left(\frac{2}{\Phi} - 1\right)CO_2$
R_{10}	$C + CO_2 \rightarrow 2\,CO$
R_{11}	$Tar + 0.48\,O_2 \rightarrow 0.92\,H_2O + CO$
R_{12}	$CNO + NO \rightarrow N_2O + CO$

Notes: Φ is a factor of a mechanism governed by particle diameter. For $d_p > 1.0$ mm $\Phi = 1$ (Zhou et al. 2011).

Table 1 Coal/biomass combustion stages in FBR as taken from (Liu et al. 2020a)	Drying	Wet coal/biomass $\rightarrow$ dry coal/biomass + moisture (H_2O)
	Pyrolysis	Dry coal/biomass $\rightarrow$ ash + volatiles + fixed carbon (char)
	Devolatilization	Volatiles $\rightarrow CH_4 + H_2O + H_2 + CO_2 + CO + H_2S + HCN + NH_3 + $ tar ($CH_{1.84}O_{0.96}$)
	Combustion	According to combustion kinetics

slightly (within 50 K). The produced tar during the combustion has often been neglected in developing the process model, due to its complexities; however, herein we account for tar combustion using reaction kinetics.

2.3 Process simulation

The developed flowsheet of the simulation, designed in Aspen Plus V11, is shown in Fig. 1. Coal, biomass, volatiles, ash, and tar were declared as non-conventional components and details were specified using HCOALGEN and DCOALIGT property methods. The COALPROC thermodynamics model was chosen for the simulation. A different approach was utilized for the tar treatment to avoid the material balance issues, arising from the fact that molecular weight of non-conventional solids is specified as 1 g/mol in Aspen Plus. Hence, tar was specified twice; a) in DEVOL ("TAR") block, as a non-conventional component produced after VM devolatilization and b) in FLUIDBED ("TAR2") as a pseudo component that is involved in kinetics governed combustion. A calculator block was added to convert "TAR" to TAR2,

with proper molecular weight of 29.2 g/mol and chemical composition of $CH_{1.84}O_{0.96}$ (Liu et al. 2020b). The CNO component involved in the reaction set was also declared as a pseudo component with a molecular weight 42.02 g/mol to eliminate incorrect properties estimations. A summary of key sub-processes used for process development is represented in Table 3.

2.4 Description of unit model

The units are specified with "C" indicates coal and with "B" indicates biomass. Since coal and biomass undergo similar process stages, the units for fuel flows are in parallel and perform equivalent tasks. The process model consists of three main units: Drying and Pyrolysis (DAPC and DAPB), Devolatilization (DEVOLATC and DEVOLATB), and Combustion (FLUIDBED). In addition, two supportive units include: Moisture separator (SEPC and SEPB) and Tar exchanger (TAREX) and two logical connectors include: Devolatilization yield calculator (C-1 and C-2) and
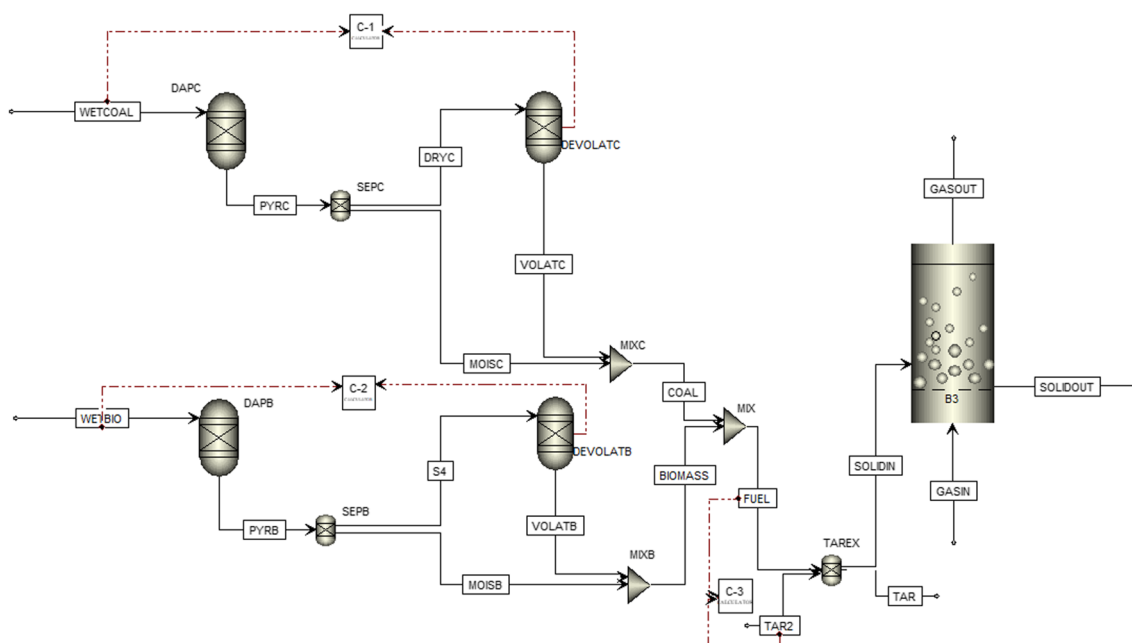

Fig. 1 The designed process model for coal/biomass combustion model in Aspen Plus v11

Table 3 Summary of main sub-processes for fuel combustion model

Sub-process	Applied block (name)	Block function
Drying and pyrolysis	RYield (DAPC & DAPB for coal & biomass)	Adjusting of mass yields according to proximate analysis
Devolatilization	RYield (DEVOL)	VM decomposition based on ultimate analyses of fuel
Combustion	FLUIDBED (B3)	Gases, char, and ash oxidation with combustion kinetics

Tar declaration calculator (C-3). The function of each block is discussed in the sections below.

DAPC & DAPB are modeled by a RYield reactor, based on proximate analysis of each component in the outlet. Since the drying and pyrolysis are assumed to have 100% conversion and occur instantaneously, all coal and biomass are converted to FC, Ash, VM, and H_2O (Serio et al. 1987). The reactors work at standard operating conditions, namely 101.325 kPa and 298 K. DEVOLATC & DEVOLATB are modeled by another RYield reactor based on the mass yield of each component using the correlation (incorporated into calculator blocks C-1 and C-2) between ultimate analysis of the fuel and composition of volatiles. Ash and FC are taken as inert in these reactor units. H_2O extracted from fuel at the drying stage is separated via SEPC and SEPB, respectively, for each fuel train and added back to the mainstream at the FLUIDBED inlet. Moisture Separator (SEPC and SEBC) were used to separate moisture from the fuel, apart from H_2O from the volatiles. Tar exchanger (TAREX) exchanged non-conventional TAR to pseudo component TAR2. Lastly, FLUIDBED is based on FLUIDBED unit with the dimensions are based on the literature and governed by combustion reactions stated in Table 2.

2.5 Reactor hydrodynamics

Selected FLUIDBED unit requires a multiple parameters adjustment. Firstly, the pressure drop over bed is defined according to Kunii and Levenspiel (1991)

$$\Delta P_b = (\rho_s - \rho_g) \times L_{mf} \times (1 - \varepsilon_{mf}) \times g/g_c$$

where ρ_s is a density of the solid particles, ρ_g is a density of gas, L_{mf} is the height of bed at minimum fluidization velocity, ε_{mf} is the voidage. Further next, minimum fluidization velocity was defined based on the Wen & Yu correlation (Kunii and Levenspiel 1991):

$$U_{mf} = \frac{d_p^2 (\rho_s - \rho_g) g}{150 \mu} \times \frac{\varepsilon_{mf}^3 \phi_s^2}{1 - \varepsilon_{mf}}, \quad Re_{p,mf} < 20$$

where ρ_g is a density of gas, μ is a viscosity of gas, and ϕ is the sphericity of particles (0.86 for sand). The Reynolds number herein is defined as:

$$Re_{p,mf} = \frac{d_p U_{mf} \rho_g}{\mu}$$

The proposed approach is generally recommended for fine particle evaluation (Kunii and Levenspiel 1991). Considering that the particle size used is typically less than 200 μm and that the density of the available sand/coal is 1.6 g/cm³, B type Geldart classification was selected. Lastly, George and Grace model was utilized for determining the transport disengagement height (TDH) and Tasirin and Geldart's model was selected to estimate the elutriation. The hydrodynamic parameters are computed and reported in Table S4 in the Supplementary Material.

3 Results and discussion

3.1 Model validation

In order to validate our process model, we begin with the data available in the recent literature. Varol et al. (2018), have performed experiments for coal and coal/biomass combustion on a fluidized bed reactor with diameter 0.1 m and height 5.1 m and operating under bed temperature of 1123 K, results of which were presented in Table S5 in Supplementary Material, along with properties of coal and biomass. Their results reveal molar fractions of the flue gases for different fuel ratios, which were taken as a basis for validating in the current model. The operating conditions and the geometry of the rector was kept the same in the current developed model, as noted above. The model was further executed for the four runs under same operating conditions and inlet flows, but with varying fuel composition (1) 3.88 kg/h of coal flow rate and 18.1 kg/h of air feed, (2) 3.08 kg/h of coal, 0.47 kg/h of biomass, and 18.5 kg/h of air feed, (3) 2.36 kg/h of coal, 1.38 kg/h of biomass, and 19.2 kg/h of air feed and (4) 1.48 kg/h of coal, 2.02 kg/h of biomass, and 22.1 kg/h of air feed. The model results in

Table 4 The emission of the gases of coal/biomass cofiring in FBR obtained from the developed process model, compared with the experiments

Run	CO$_2$ (%vol) exp[a]	CO$_2$ (%vol) Model	CO (ppm) exp[a]	CO (ppm) Model	NO (ppm) exp[a]	NO (ppm) Model	SO$_2$ (ppm) exp[a]	SO$_2$ (ppm) Model
1	15.5 ± 0.8	17.7	86 ± 12	80	131 ± 13	127	977 ± 130	938
2	15.5 ± 0.8	15.9	59 ± 5	60	144 ± 13	140	806 ± 172	808
3	15.3 ± 0.7	16.2	30 ± 7	35	120 ± 7	125	410 ± 87	448
4	15.4 ± 1.2	13.4	56 ± 15	48	120 ± 19	131	303 ± 83	304

Notes: a based on the experiments presented by Varol et al. (2018)

terms of CO_2, CO, NO, SO_2 emissions were compared with the experimental data and are presented in Table 4.

It can be noticed that the model results are in a reasonable agreement with the experimental data. The mean-absolute deviation between the emissions of CO_2, CO, NO, and SO_2 are 1.4%, 5.0 ppm, 6.0 ppm, and 20 ppm, respectively. Given that results are comparable, the model further was used to observe behavior of coal and coal/biomass fuel combustion under different conditions based on the low grade bituminous Ekibastuz coal and organic MSW samples.

3.2 Implementation on Ekibastuz coal and local MSW

In our previous work (Saparov et al. 2021), properties of the Ekibastuz coal were measured according to ASTM requirements and modeled under combustion environment using basic kinetics. This type of bituminous coal is characterized as low-quality due to the high ash content of up to 40%. Herein, we evaluate its potential, in terms of gas emissions, for the fluidized bed co-combustion with biomass. The parameters for the biomass, particularly taking the organic fraction of MSW of Nur-Sultan, Kazakhstan, were retrieved from our previous work (Tokmurzin et al. 2020). The density of the particles was 1.8 g/cm^3 and 0.31 g/cm^3, for Ekibastuz coal and organic fraction of MSW. Mean particle size distribution was in range of 6000–8000 microns for both fuels. The detailed information of both coal and biomass thermal characteristics is incorporated in Table 5.

Evaluation of the thermo-chemical properties of the biomass (organic fraction of MSW collected in capital city of Kazakhstan) include ultimate, proximate analysis, and evaluation of the calorific value. Further, UNICUBE®

micro elemental analyzer was used for ultimate analysis. Proximate analysis was conducted in accordance with ISO 18134-3:2015(E), ISO 18122:2015(E), ISO 18123:2015(E) standards for solid waste fuels to estimate moisture, volatile matter, carbon, and ash content of the fuel. Bomb calorimeter (Etalon®) was implemented for the calorific value determination.

As can be observed, biomass has a relatively higher volatile matter content than coal while both ash and fixed carbon abundance is halved. In order to model Ekibastuz coal and co-firing of the biomass obtained from the local MSW, the regression model was applied to obtain constituents of the volatile matter (results shown in Table S6 in Supplementary Material). Data from regression analysis was used in devolatilization units (DEVOLATC and DEVOLATB) using the RYield reactor to specify mass yields of devolatilization products. The designed process model was tested again with combustion of only Ekibastuz coal and the emissions of the four components were compared with those observed from the experiments of (Saparov et al. 2021), wherein the reactor height was 7 m, diameter of 0.18 m and operating temperature of 1173 K (Table S7 in Supplementary Material), and as reported by us earlier. The results (Table 6) show a good agreement between the model prediction and the experiments. This further supports our model parameters and its flexibility and resilience in varying operating conditions, fuel changes, and geometry of the reactor.

While the predicted concentrations for $CO_2/O_2/H_2O/N_2O$ gases were in a good agreement, SO_2 concentration was approximately two times lower than the experimental data. There are two key factors that can affect the SO_2 emissions in the developed model: In our model, the fuel devolatilization was carried based on the results of the fuel's ultimate analysis, with the final composition of the volatile matter, as proposed by Serio et al. (1987). The method implies that sulphur in fuel goes completely in the form of H_2S in the 'pyrolysis' block. However, in the combustion experiments, a fraction of sulfur remains as a solid constituent of the char and thermally decomposes during the char combustion (Jerzak et al. 2020). This implies that a long residence time is required for the complete fuel-S oxidation. As observed from Table 2, the reaction set

Table 5 Fuel properties for Ekibastuz coal and organic fraction of the MSW. Adapted from (Tokmurzin et al. 2020; Saparov et al. 2021)

Item	Ekibastuz coal	Organic biomass from MSW
Proximate analysis (wt% as received)		
FC	40.21	23.35
VM	21.55	59.35
Ash	38.24	13.90
Moisture	1.31	3.40
Ultimate analysis (wt% dry basis)		
C	48.10	46.16
H	3.10	6.23
N	1.40	4.18
S	0.60	0.26
O	8.56	43.17
HHV (kJ/kg, as fired)		
	19,400	17,770

Table 6 Validation of the model based on flue gas composition for Ekibastuz coal combustion

Component	Experiment	Simulation
CO_2 (%)	12–15	12.8
O_2 (%)	3.5–5	5.2
H_2O (%)	4–6	4.8
SO_2 (ppm)	350–450	157
N_2O (ppm)	80–120	108

involved in the fuel combustion process incorporates only one reaction for the H_2S oxidation with a further formation of the SO_2. Another reason for the observed deviation in SO_2 composition is that Saparov et al. (2021), experimented on a semi-industrial circulating fluidized bed reactor (CFBR), whereas in the current model solids recirculation was not considered. In CFBR ash, char, and the bed material (inert sand) from the top of the riser is passed on to the cyclone, wherein the dense particles were separated from flue gases and were directed to the dense zone of the reactor for increased residence time and complete combustion. In this context, our work (on bubbling bed fluidized reactor) is not in complete correspondence with the earlier experiments of Saparov et al. (2021). However, for biomass, the predominant fuel-S content is released during the devolatilization at low temperatures (Knudsen et al. 2004). Hence our model is able to well-predict SO_2 emissions for all cases with biomass combustion, as shown in Table 4.

Sensitivity analyses were further performed for varying biomass fraction in blend fuel and operating temperature to observe the behavior of Ekibastuz coal and biomass in terms of organic fraction of MSW. The geometry of the reactor was kept the same as those of Varol et al. (2018). A series of runs were made based on varying biomass composition and air flow rate. The total flow rate of the fuel was kept at 4 kg/h, and the temperature and pressure were at 298 K and 101.325 kPa, whereas air flow rate was kept constant at 25 kg/h at 873 K and 101.325 kPa.

The predicted emission results from the model were plotted in terms of emissions of gases (Fig. 2). Figure 2 shows the effect of varying biomass fraction at constant reactor temperature of 1073 K, 101.325 kPa. In performing the sensitivity analysis, air flow rate was kept constant at 25 kg/h in all six runs. The proportion of biomass was increased from 2.5% to 97.5% (0.1 kg/h to 3.9 kg/h of biomass) to examine the flue gas content.

Lastly, the effect of combustion temperature on emissions was evaluated based on the process model. The temperature of the fluidized bed was changed from 1073 to 1223 K keeping the air flow at 25 kg/h. Biomass/coal ratio was gradually changed from 1:4 to 1:1, maintaining the total fuel flow at 4 kg/h, with biomass fraction changing from 0.8 to 2 kg/h. Next, we discuss on the emission profiles with varying biomass and temperature. A lower limit of the biomass proportion was set to 1:4 of the overall fuel weight, as below this limit no significant changes were observed in the flue gas compositions within the operating parameters.

3.3 NO emissions

Figures 2a and 3a showed a slight increase of NO molar fraction, when the mass fraction of biomass extends in the blend fuel. The same behavior is detected with a temperature increase. However, after 1173 K in all analyzed B/C ratios NO content starts to decrease. As stated in literature (Nordin 1994; Demirbas 2004; Akram et al. 2013), the fluidized bed reactors typically operate at temperatures between 1073 and 1198 K, thus the formation of the thermal and/or prompt NO gases can be neglected. Hence, the fuel nitrogen is predominant for analyzed cases. The above-mentioned trend can be justified by the intensified formation of NH_3 and HCN (devolatilization stage) that depends on the volatile content in fuel and furnace temperature (Jensen et al. 1995). Further intensification of the combustion process is observed at higher furnace temperatures and subsequently, the radical production is increased resulting in higher conversion of fuel nitrogen in NO (Kilpinen and Hupa 1991; Duan et al. 2015; Qin et al. 2019). In addition, the highest values for NO concentrations were 566 ppm (Fig. 3a) and 392 ppm (Fig. 2a) which is a reasonable according to the literature (Werther et al. 2000; Nussbaumer and Hustad 1997) values
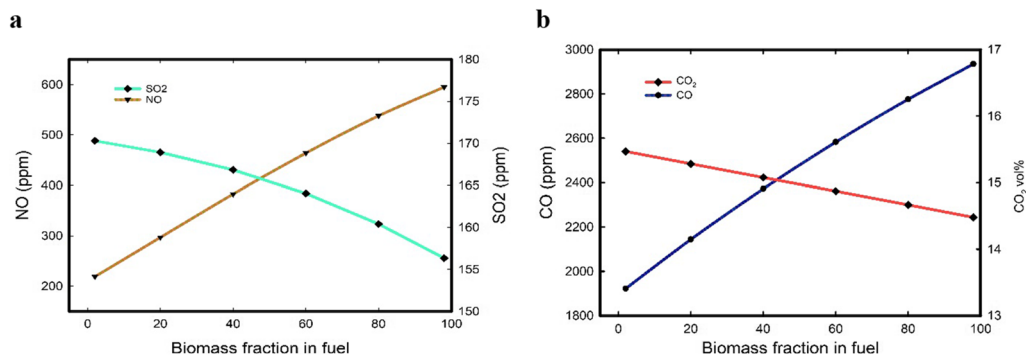

Fig. 2 **a** Effect of biomass fraction on SO_2 (right scale) and NO (left scale); **b** CO (left scale) and CO_2 (right scale) composition in flue gas at 1073 K, 101.325 kPa, 25 kg/h air flow rate
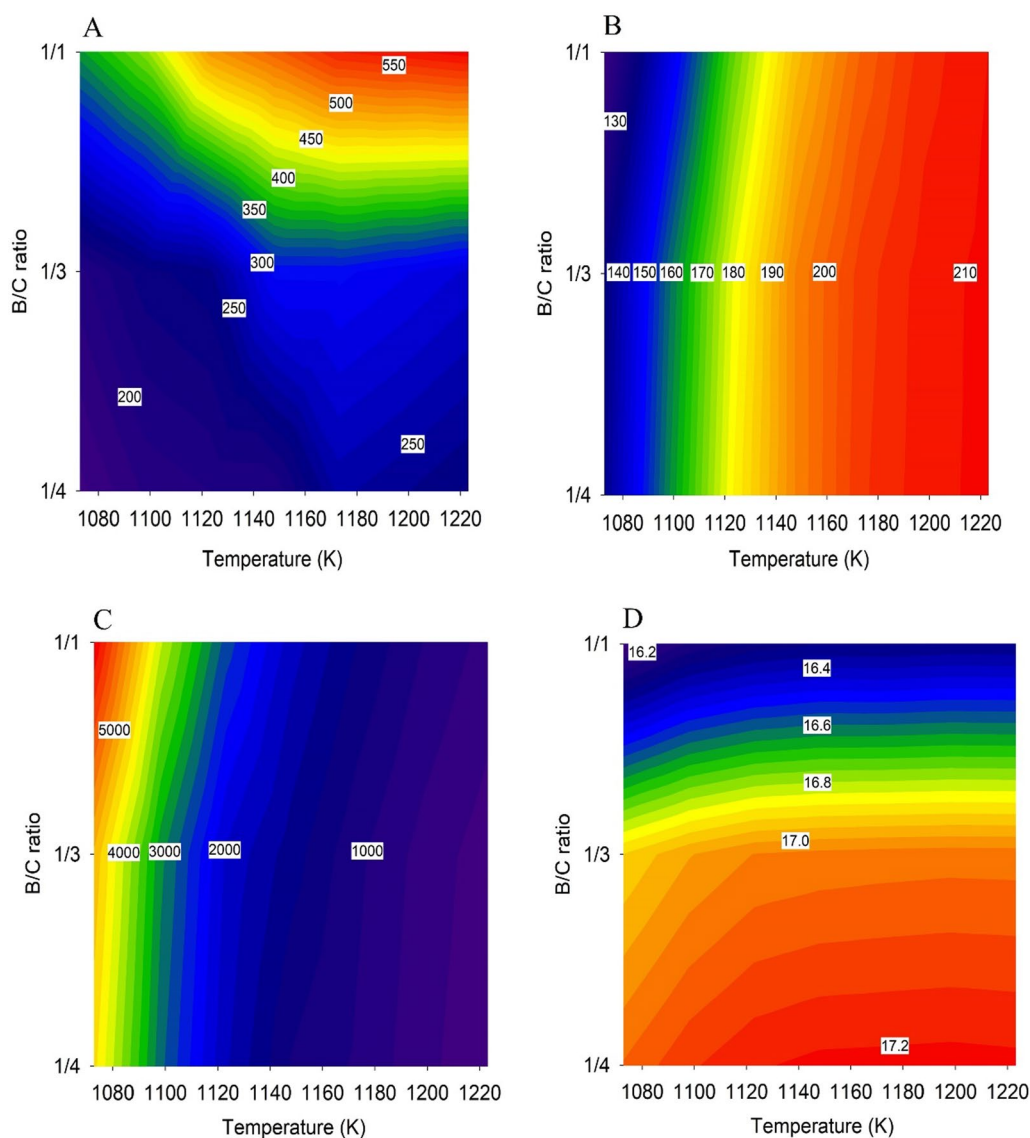
Fig. 3 Effect of operating temperature on **a** NO, **b** SO_2, **c** CO and **d** CO_2 composition at total feed of 4 kg/h and air flow rate of 25 kg/h with different Biomass/Coal (B/C) ratio

that suggest that lab-scale and semi-industrial FBR can generate up to 1000 mg/m^3 of NO$_x$ emissions.

3.4 SO_2 emissions

The investigation of SO_2 concentration revealed an increase with increasing reactor temperature (Fig. 3b); however, the results at constant temperature (Fig. 2a) had demonstrated a minor decrease and comparatively SO_2 concentrations are very low even at relatively high biomass fraction in fuel mixture. A similar trend was reported by Khan et al. (2009) wherein the authors have underlined three possible reasons: (1) total sulfur content of the fuel mixture decreased when the biomass content was extended(Miles et al. 1996;

Kuznetsov et al. 2021), particularly, in the tested biomass is two-times lower compared with coal; (2) the presence of CaO and MgO in biomass ash enhanced the absorption of sulfur (Fuertes et al. 1992) and (3) enhanced kinetics of H_2S combustion (Suksankraisorn et al. 2004) could affect the SO_2 molar fraction in flue gases. The maximum values of SO_2 emission were observed to be 145 ppm (Fig. 2a) and 210 ppm (Fig. 3b).

3.5 CO emissions

Figures 2a and 3c indicate the sharp growth of the CO content in flue gas with increased biomass content in the blend fuel. This increase is attributed to the fact that the

MSW has a higher content of volatile gases in the riser, which contributes significantly to the CO concentration (Gungor 2013; Xie et al. 2017). Earlier literature (Khan et al. 2009) underlined that short freeboard and insufficient residence time are the reasons for high CO concentration during the operation on small-scale fluidized bed reactors. Analysis of the contour plot (Fig. 3c) highlights the trend of CO emissions decrease with an increase of the furnace temperature, particularly beyond 1100 K. To optimize the CO emissions, it is recommended to design a FBRs with a long riser and supply extra oxygen as it was mentioned in the literature (Williams et al. 2001; Demirbaş 2005). Moreover, the maximum value for CO concentrations observed were 2657 ppm (Fig. 2b) and 6180 ppm (Fig. 3c).

3.6 CO_2 emissions

The results interestingly reveal that CO_2 concentration does not vary significantly with a change in composition of the fuel (Fig. 2a). These results are consistent with those obtained by Varol et al. (Varol et al. 2018), wherein the authors have observed that biomass concentration in blend fuel combustion under air conditions do not result in notable changes in CO_2 emissions. Lastly, the change of CO_2 concentration with temperature is demonstrated in Fig. 3d. The compositions were in the range of 16.0%–17.1%, because of the low air flow rate. The trend of increasing CO_2 emissions at higher temperatures for Ekibastuz coal is in agreement with a previous study presented by Saparov et al. (2021). CO_2 concentration reduces with an increase of biomass fraction and this trend justifies the potential of MSW conversion for GHG reduction. Moreover, at temperatures lower than 1100 K the rate of CO_2 concentration growth is lower than at higher temperatures. The highlighted pattern is a result of interconnection between the rapid decrease of CO and increase of CO_2 concentration in the flue gases and has been discussed earlier (Khan et al. 2009; Bhuiyan et al. 2018; Saparov et al. 2021).

The optimal parameters for FBR can be proposed based on the sensitivity analysis results. In the selected range of temperature, the rate of CO decrease is faster than the rate of NO increase while the SO_2 concentration does not change significantly. Thus, it can be recommended to keep the optimal reactor temperature at 1148 K, because among the examined range, the lowest concentration of CO was observed despite the relatively high NO concentration. CO_2 and SO_2 emissions did not change significantly at the proposed FBR operating temperature. Moreover, the analysis of the flue gas composition at different blend fuel ratios demonstrated that at 1/3 and 1/1 biomass/coal ratios: (1) CO concentration is 26% and 60%, and (2) NO is 50% and 160% higher than in case when biomass presence not exceed 20% of total feed. Thus, for the FBR with abovementioned geometry, the optimal operation temperature is 1148 K while the recommended B/C ratio is 1/4.

4 Conclusions

A versatile model has been established in Aspen Plus for co-firing coal and biomass in a fluidized bed reactor. The flexibility of the model has been validated primarily using the recent experiments of co-firing of Spanish lignite and wood-pellets and further by our previous experiments on the low-quality Ekibastuz coal. The model has numerous novel features including (1) the composition of volatiles which was calculated using the theory of the functional-group dependence on the ultimate analysis for coal, (2) Adaptation of the FLUIDBED unit in Aspen plus to include hydrodynamics, which has often been neglected, along with the reaction kinetics, and (3) detailed kinetics of twelve reactions were used for the simulation of the combustion process during co-firing. While the model works well in predicting the flue emissions, it needs to be further developed to account for heat transfer within the system. Evaluation of the heat generation and its dependence on the moisture content is an interesting field to explore further. Lastly, the sensitivity analysis presented on co-firing of local biomass and Ekibastuz coal provides detailed guidelines for designing optimum experiments.

Declarations

References

Adamczyk WP, Kozołub P, Klimanek A et al (2015) Numerical simulations of the industrial circulating fluidized bed boiler under air- and oxy-fuel combustion. Appl Therm Eng 87:127–136. https://doi.org/10.1016/j.applthermaleng.2015.04.056

Aghaalikhani A, Schmid JC, Borello D et al (2019) Detailed modelling of biomass steam gasification in a dual fluidized bed gasifier with temperature variation. Renew Energy 143:703–718. https://doi.org/10.1016/j.renene.2019.05.022

Akram M, Garwood R, Tan CK (2013) Effect of fuel characteristics and operating conditions on NO_x emissions during fluidised bed combustion of high moisture biomass with coal. J Energy Inst 86:177–186. https://doi.org/10.1179/1743967113Z.00000000062

Awasthi A, Bhaskar T (2019) Combustion of lignocellulosic biomass, 2nd edn. Elsevier Inc., Amsterdam

Bhuiyan AA, Blicblau AS, Islam AKMS, Naser J (2018) A review on thermo-chemical characteristics of coal/biomass co-firing in industrial furnace. J Energy Inst 91:1–18. https://doi.org/10.1016/j.joei.2016.10.006

Bi H, Wang C, Lin Q, Jiang X, Jiang C, Bao L (2021) Pyrolysis characteristics, artificial neural network modeling and environmental impact of coal gangue and biomass by TG-FTIR. Sci Total Environ 751:142293. https://doi.org/10.1016/j.scitotenv.2020.142293

Demirbas A (2004) Combustion characteristics of different biomass fuels. Prog Energy Combust Sci 30:219–230. https://doi.org/10.1016/j.pecs.2003.10.004

Demirbaş A (2005) Biomass co-firing for boilers associated with environmental impacts. Energy Sources 27:1385–1396. https://doi.org/10.1080/009083190523217

Duan L, Duan Y, Zhao C, Anthony EJ (2015) NO emission during co-firing coal and biomass in an oxy-fuel circulating fluidized bed combustor. Fuel 150:8–13. https://doi.org/10.1016/j.fuel.2015.01.110

Dwivedi KK, Chatterjee PK, Karmakar MK, Pramanick AK (2019) Pyrolysis characteristics and kinetics of Indian low rank coal using thermogravimetric analysis. Int J Coal Sci Technol 6:102–112. https://doi.org/10.1007/s40789-019-0236-7

Fedorov AV, Dubinin YV, Yeletsky PM et al (2021) Combustion of sewage sludge in a fluidized bed of catalyst: ASPEN PLUS model. J Hazard Mater 405:124196. https://doi.org/10.1016/j.jhazmat.2020.124196

Fuertes AB, Artos V, Pis JJ et al (1992) Sulphur retention by ash during fluidized bed combustion of bituminous coals. Fuel 71:507–511. https://doi.org/10.1016/0016-2361(92)90147-G

Gu J, Shao Y, Zhong W (2020) 3D simulation on pressurized oxy-fuel combustion of coal in fluidized bed. Adv Powder Technol 31:2792–2805. https://doi.org/10.1016/j.apt.2020.05.005

Gungor A (2013) Simulation of co-firing coal and biomass in circulating fluidized beds. Energy Convers Manage 65:574–579. https://doi.org/10.1016/j.enconman.2012.09.023

Hu Y, Wang J, Tan CK et al (2018) Coupling detailed radiation model with process simulation in Aspen Plus: a case study on fluidized bed combustor. Appl Energy 227:168–179. https://doi.org/10.1016/j.apenergy.2017.08.030

IEA (2018) World energy outlook 2018: highlights. Int Energy Agency 1:1–661

Jensen A, Johnsson JE, Andries J et al (1995) Formation and reduction of NO_x in pressurized fluidized bed combustion of coal. Fuel 74:1555–1569. https://doi.org/10.1016/0016-2361(95)00155-X

Jerzak W, Kalicka Z, Kawecka-Cebula E, Kuźnia M (2020) SO_2 emission characteristics of bituminous coal, lignite, and its blends with cedar nut shells under O_2/N_2 and O_2/CO_2 combustion environments in a bubbling fluidized bed. Combust Sci Technol 192:560–574. https://doi.org/10.1080/00102202.2019.1583220

Kerimray A, Suleimenov B, de Miglio R et al (2018) Long-term climate change mitigation in Kazakhstan in a post Paris agreement context, pp 297–314

Khan AA, de Jong W, Jansens PJ, Spliethoff H (2009) Biomass combustion in fluidized bed boilers: potential problems and remedies. Fuel Process Technol 90:21–50. https://doi.org/10.1016/j.fuproc.2008.07.012

Kilpinen P, Hupa M (1991) Homogeneous N2O chemistry at fluidized bed combustion conditions: a kinetic modeling study. Combust Flame 85:94–104. https://doi.org/10.1016/0010-2180(91)90179-F

Knudsen JN, Jensen PA, Lin W et al (2004) Sulfur transformations during thermal conversion of herbaceous biomass. Energy Fuels 18:810–819. https://doi.org/10.1021/ef034085b

Kommalapati RR, Hossan I, Botlaguduru VSV et al (2018) Life cycle environmental impact of biomass co-firing with coal at a power plant in the greater Houston area. Sustainability (switzerland) 10:2193. https://doi.org/10.3390/su10072193

Kumar H, Mohapatra SK, Singh RI (2018) Review on CFD modelling of fluidized bed combustion systems based on biomass and co-firing. J Inst Eng (india): Ser C 99:449–474. https://doi.org/10.1007/s40032-017-0361-2

Kunii D, Levenspiel O (1991) Fluidization Engineering (2nd ed). Butterworth-Heinemann. ISBN 9780080506647. https://doi.org/10.1016/B978-0-08-050664-7.50007-X

Kuznetsov GV, Nyashina GS, Strizhak PA, Valiullin TR (2021) Experimental research into the ignition and combustion characteristics of slurry fuels based on dry and wet coal processing waste. J Energy Inst 97:213–224. https://doi.org/10.1016/j.joei.2021.05.001

Lawal AI, Aladejare AE, Onifade M et al (2021) Predictions of elemental composition of coal and biomass from their proximate analyses using ANFIS, ANN and MLR. Int J Coal Sci Technol 8:124–140. https://doi.org/10.1007/s40789-020-00346-9

Liu Q, Zhong W, Gu J, Yu A (2020a) Three-dimensional simulation of the co-firing of coal and biomass in an oxy-fuel fluidized bed. Powder Technol 373:522–534. https://doi.org/10.1016/j.powtec.2020.06.092

Liu Q, Zhong W, Yu H et al (2020b) Experimental studies on the emission of gaseous pollutants in an oxy-fuel-fluidized bed with the cofiring of coal and biomass waste fuels. Energy Fuels. https://doi.org/10.1021/acs.energyfuels.0c01061

Merrick D (1984) Coal combustion and conversion technology. Coal Combust Convers Technol. https://doi.org/10.1016/0016-2361(85)90068-7

Miles TR, Miles TR, Baxter LL et al (1996) Boiler deposits from firing biomass fuels. Biomass Bioenerg 10:125–138. https://doi.org/10.1016/0961-9534(95)00067-4

Nordin A (1994) Chemical elemental characteristics of biomass fuels. Biomass Bioenerg 6:339–347. https://doi.org/10.1016/0961-9534(94)E0031-M

Nussbaumer T, Hustad JE (1997) Overview of biomass combustion. In: Bridgwater AV, Boocock DGB (eds) Developments in thermochemical biomass conversion. Springer, Dordrecht, pp 1229–1243. https://doi.org/10.1007/978-94-009-1559-6_98

Peters J, May J, Ströhle J, Epple B (2020) Flexibility of CFB combustion: an investigation of co-combustion with biomass and RDF at part load in pilot scale. Energies (basel) 13:4665. https://doi.org/10.3390/en13184665

Qin J, Zhao R, Chen T et al (2019) Co-combustion of municipal solid waste and coal gangue in a circulating fluidized bed combustor. Int J Coal Sci Technol 6:218–224. https://doi.org/10.1007/s40789-018-0231-4

Roni MS, Chowdhury S, Mamun S et al (2017) Biomass co-firing technology with policies, challenges, and opportunities: A global review. Renew Sustain Energy Rev 78:1089–1101. https://doi.org/10.1016/j.rser.2017.05.023

Saparov A, Kulmukanova L, Mostafavi E et al (2021) Development and validation of a novel process model for fluidized bed combustion: application for efficient combustion of low-grade coal. Can J Chem Eng 99:1510–1519. https://doi.org/10.1002/cjce.23896

Serio MA, Hamblen DG, Markham JR, Solomon PR (1987) Kinetics of volatile product evolution in coal pyrolysis: experiment and theory. Energy Fuels 1:138–152. https://doi.org/10.1021/ef00002a002

Sher F, Pans MA, Sun C et al (2018) Oxy-fuel combustion study of biomass fuels in a 20 kWth fluidized bed combustor. Fuel 215:778–786. https://doi.org/10.1016/j.fuel.2017.11.039

Suksankraisorn K, Patumsawad S, Vallikul P et al (2004) Co-combustion of municipal solid waste and Thai lignite in a fluidized bed. Energy Convers Manage 45:947–962. https://doi.org/10.1016/S0196-8904(03)00187-0

Tokmurzin D, Kuspangaliyeva B, Aimbetov B et al (2020) Characterization of solid char produced from pyrolysis of the organic fraction of municipal solid waste, high volatile coal and their blends. Energy 191:116562. https://doi.org/10.1016/j.energy.2019.116562

UNFCCC (2011) Intended nationally determined contribution—submission the Republic of Kazakhstan

Varol M, Symonds R, Anthony EJ et al (2018) Emissions from co-firing lignite and biomass in an oxy-fired CFBC. Fuel Process Technol 173:126–133. https://doi.org/10.1016/j.fuproc.2018.01.002

Werther J, Saenger M, Hartge EU et al (2000) Combustion of agricultural residues. Prog Energy Combust Sci 26:1–27. https://doi.org/10.1016/S0360-1285(99)00005-2

Williams A, Pourkashanian M, Jones JM (2001) Combustion of pulverised coal and biomass. Prog Energy Combust Sci 27:587–610. https://doi.org/10.1016/S0360-1285(01)00004-1

Wu Y, Liu D, Ma J, Chen X (2017) Three-dimensional Eulerian–Eulerian simulation of coal combustion under air atmosphere in a circulating fluidized bed combustor. Energy Fuels 31:7952–7966. https://doi.org/10.1021/acs.energyfuels.7b01084

Xie J, Zhong W, Jin B et al (2014) Three-dimensional Eulerian–Eulerian modeling of gaseous pollutant emissions from circulating fluidized-bed combustors. Energy Fuels 28:5523–5533. https://doi.org/10.1021/ef501095r

Xie J, Zhong W, Shao Y et al (2017) Simulation of combustion of municipal solid waste and coal in an industrial-scale circulating fluidized bed boiler. Energy Fuels 31:14248–14261. https://doi.org/10.1021/acs.energyfuels.7b02693

Yang X, Liu B, Song W, Lin W (2011) Process simulation of emission and control for NO and N2O during coal combustion in a circulating fluidized bed combustor based on Aspen Plus. Energy Fuels 25:3718–3730. https://doi.org/10.1021/ef200721y

Zhou W, Zhao CS, Duan LB et al (2011) Two-dimensional computational fluid dynamics simulation of coal combustion in a circulating fluidized bed combustor. Chem Eng J 166:306–314. https://doi.org/10.1016/j.cej.2010.09.048

Žnidarčič A, Katrašnik T, Zsély IG et al (2021) Sewage sludge combustion model with reduced chemical kinetics mechanisms. Energy Convers Manage 236:114073. https://doi.org/10.1016/j.enconman.2021.114073